

**Molecular Cell, Volume 70**

**Supplemental Information**

**Structural Basis of Splicing Modulation**

**by Antitumor Macrolide Compounds**

**Constantin Cretu, Anant A. Agrawal, Andrew Cook, Cindy L. Will, Peter Fekkes, Peter G. Smith, Reinhard Lührmann, Nicholas Larsen, Silvia Buonamici, and Vladimir Pena**



Figure S2

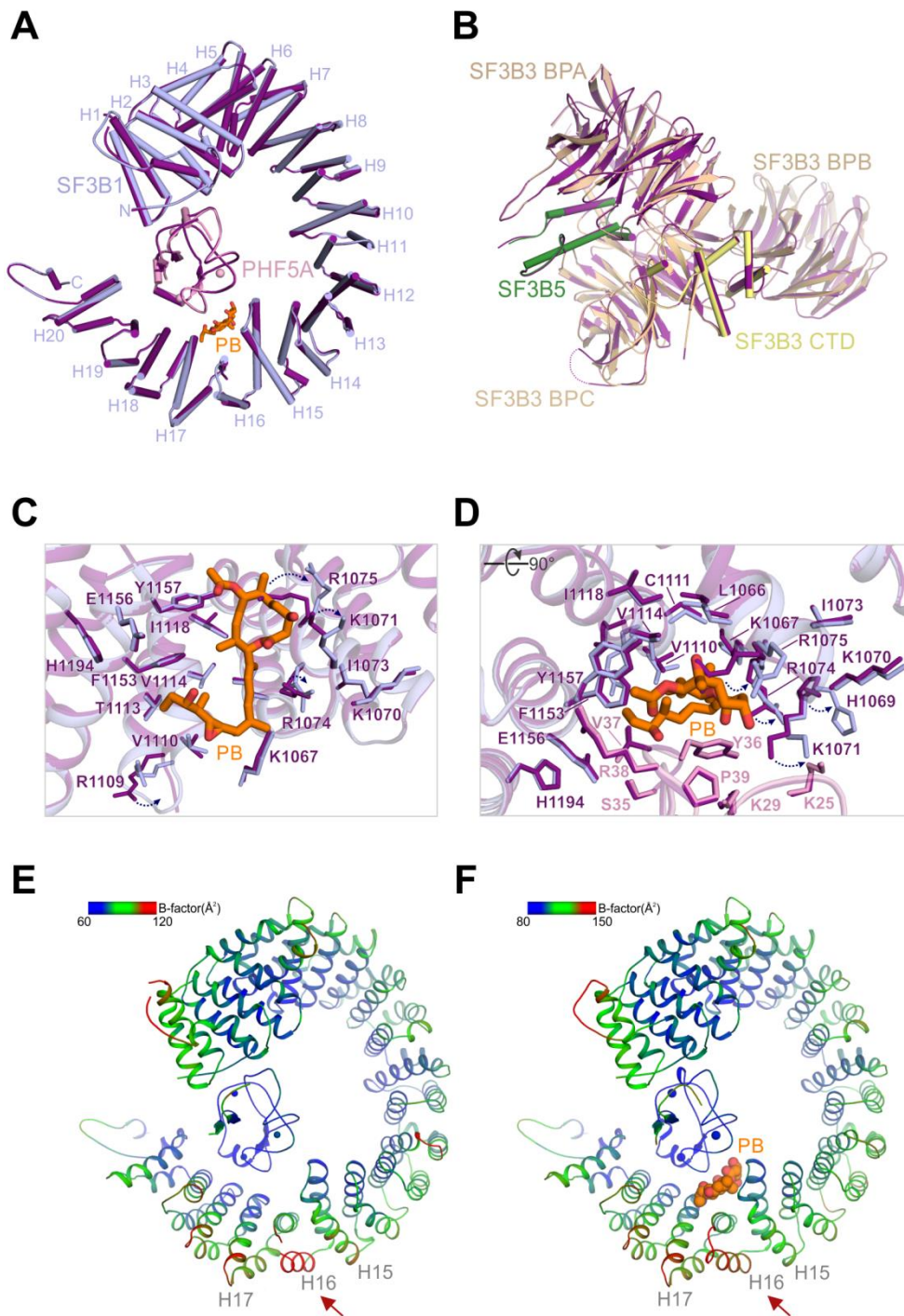
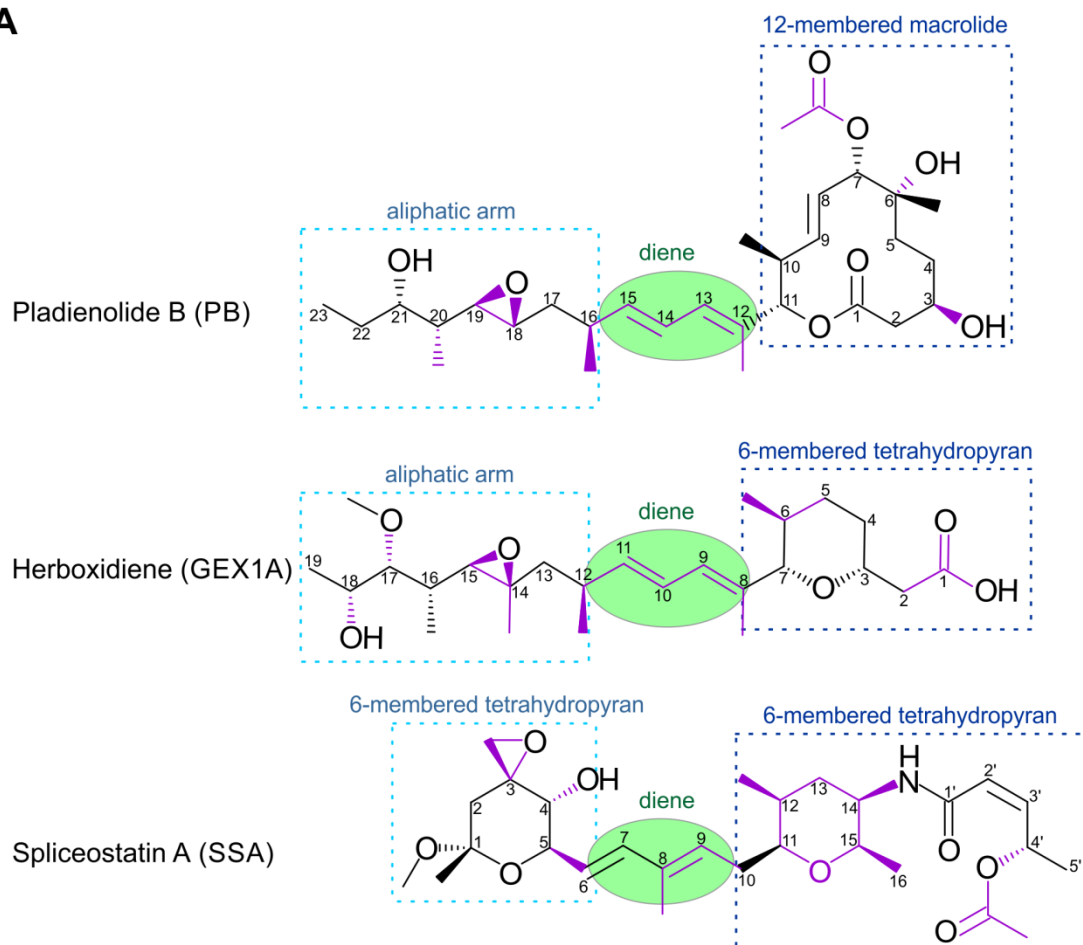
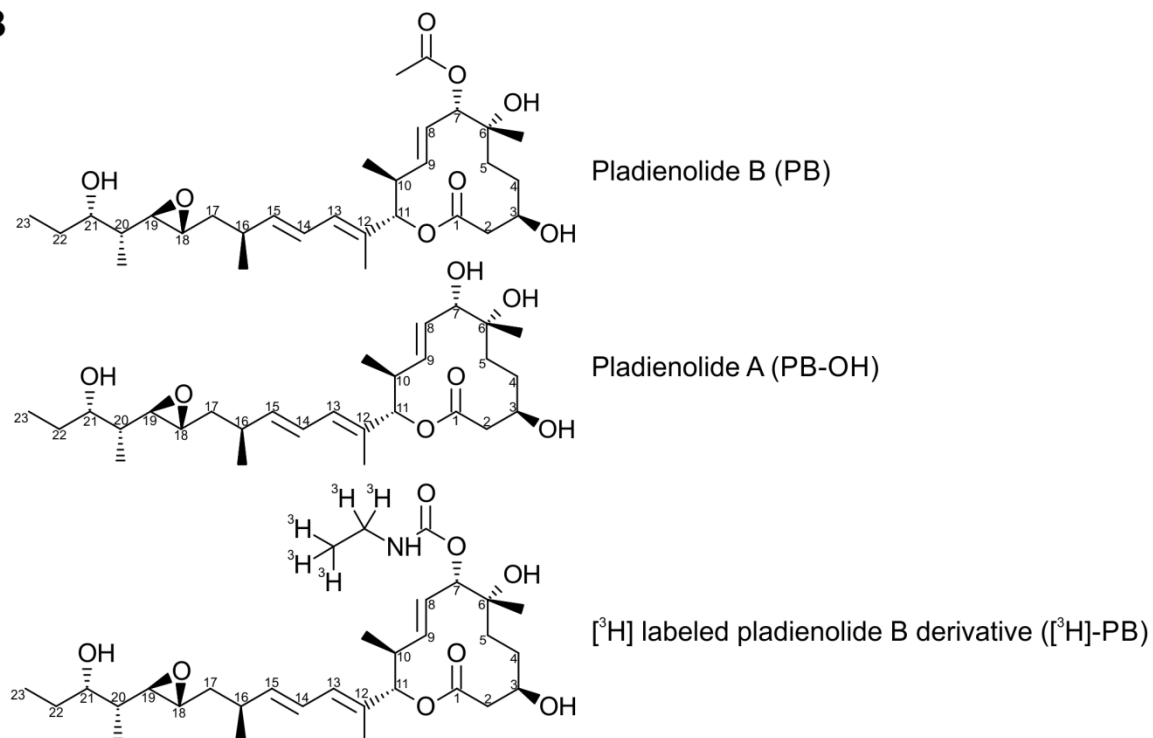


Figure S3

A



B



**Figure S4**

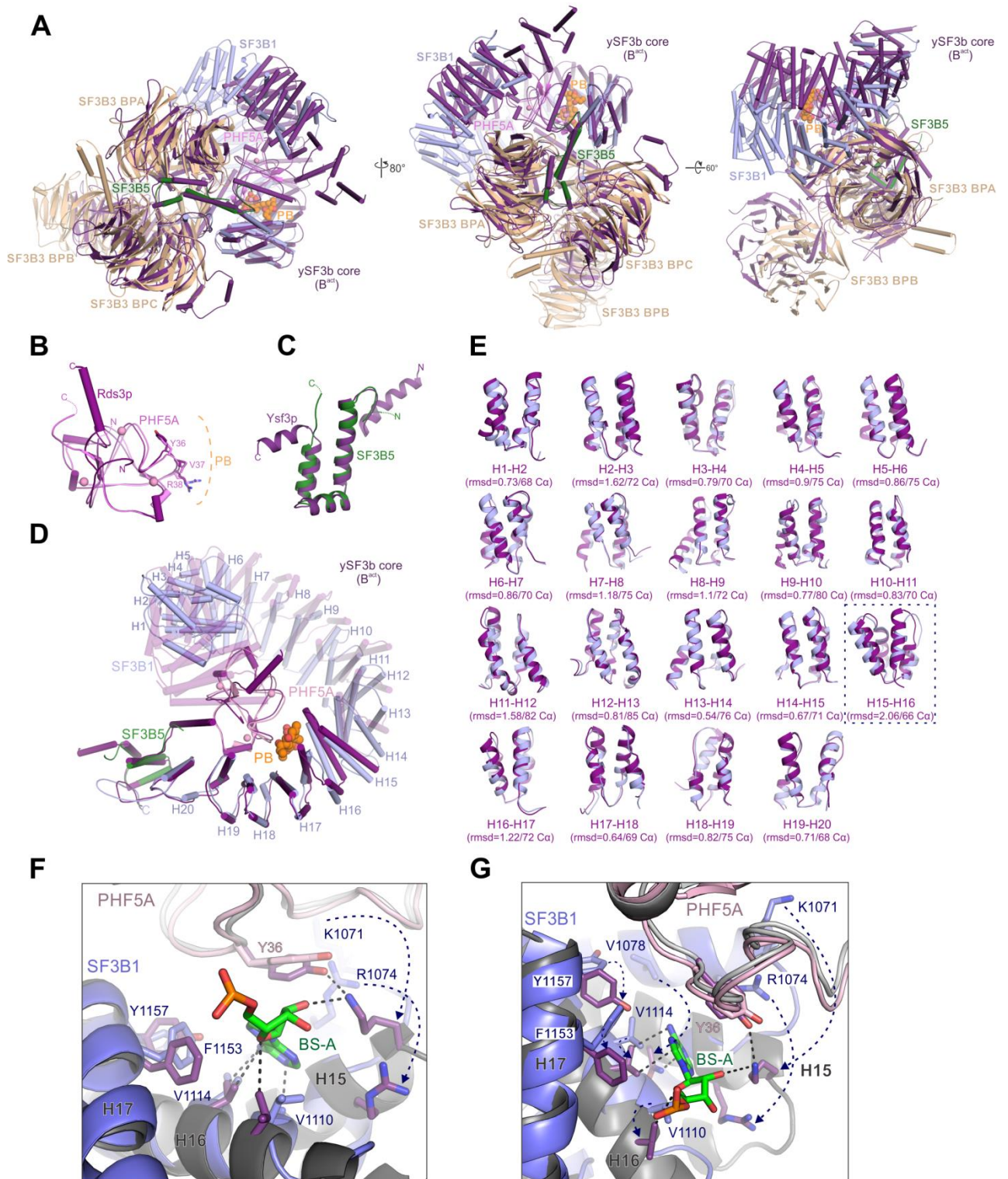


**Figure S5**

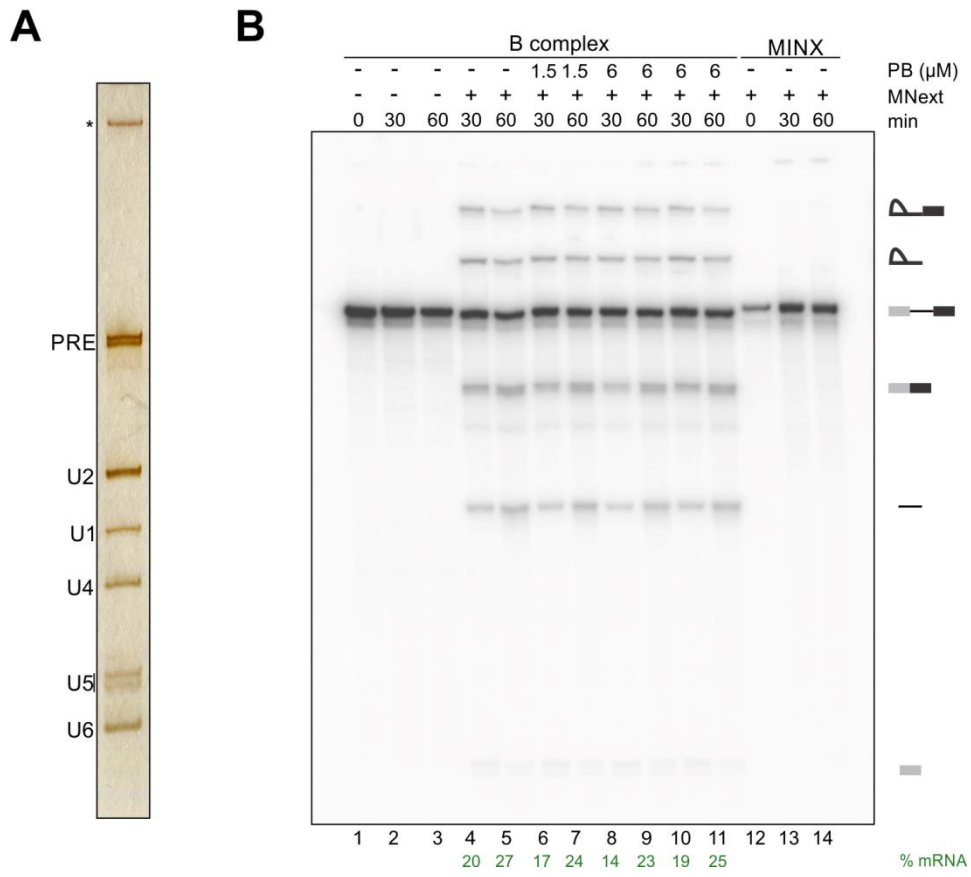
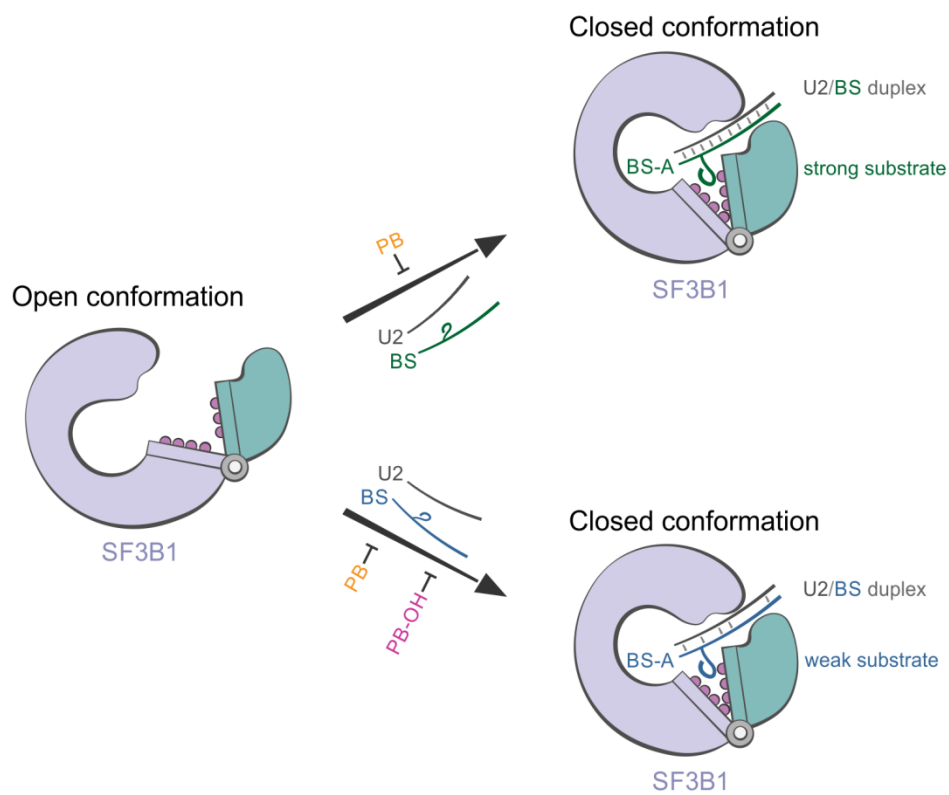


Figure S6

A

Ad2-derived splicing substrates	Sequence (3' splice site)	PB IC <sub>50</sub> (nM)	PB-OH IC <sub>50</sub> (nM)	Fold change
Enhanced BS (Ad2.1)	-32   -14   -1 TCATACTT <b>AA</b> TCCTGTCCC <b>TTTTTTT</b> CCACAG	19	-	>100
Wild-type (Ad2)	-32   -14   -1 TCATACTT <b>A</b> TCCTGTCCC <b>TTTTTTT</b> CCACAG	18	1589	88.3
Strong BS/weak PPT (Ad2.12)	-32   -14   -1 TCATACTT <b>A</b> TCCTGTCCC <b>CCCCCCCC</b> CCACAG	19	1235	65
Weak BS/strong PPT (Ad2.11)	-32   -14   -1 TCATA <b>AGTTA</b> TCCTGTCCC <b>TTTTTTT</b> CCACAG	22	224	10.2
Weak BS/weak PPT (Ad2.15)	-32   -14   -1 TCATA <b>AGTTA</b> TCCTGTCCC <b>CCCCCCCC</b> CCACAG	18	158	8.8
Decoy BS/strong PPT (Ad2.2)	-32   -14   -1 <b>TACTACTT</b> A <b>A</b> TCCTGTCCC <b>TTTTTTT</b> CCACAG	29	54	1.9

B



**Figure S1. Crystal structure of an engineered human SF3B core in complex with pladienolide B (PB). Related to Figure 1.**

(A) Coomassie-stained SDS-PAGE analysis of an engineered human SF3B core complex, reconstituted by co-expression in insect cells, after size-exclusion chromatography. SF3B3 (lacking residues 1068-1085), SF3B1 (residues 453-1304), PHF5A (residues 1-98), and SF3B5 (full-length) appear to be present in stoichiometric amounts. (B) Scintillation proximity assays of the human SF3B core in the presence of a tritiated PB derivative ( $[^3\text{H}]$ -PB) and unlabelled PB or PB-OH as competitors. The engineered SF3B core binds  $[^3\text{H}]$ -PB suggesting that the minimal complex contains an intact PB binding site ( $\text{IC}_{50} = 130 \text{ nM}$  for PB and  $\text{IC}_{50} = 1070 \text{ nM}$  for PB-OH). (C) Electron density maps of the PB ligand calculated from the refined structure. Residual  $mF_o - DF_c$  (contoured at  $3\sigma$ ) and polder (contoured at  $6\sigma$ ) omit maps are displayed next to a  $2mF_o - DF_c$  map (contoured at  $1\sigma$ ). The PB ligand is depicted as orange sticks. (D) Electron density map of SF3B1 at the PB binding site. The  $2mF_o - DF_c$  map (grey mesh,  $1\sigma$ ) is displayed around SF3B1 (light blue) and the PB ligand is shown as orange sticks (see also Figure 1B). (E), Electron density map of the SF3B1-PHF5A PB binding tunnel. The  $2mF_o - DF_c$  map (grey mesh,  $1\sigma$ ) is shown around SF3B1 (light blue), PHF5A (pink), and PB (orange). Key residues lining the SF3B1-PHF5A tunnel are depicted as sticks. (F), (G) Selenium marker sites validate the residue register of the SF3B core structure. Selenium sites were identified using SAD log-likelihood gradient maps and are shown as yellow spheres. The modeled methionine side chains are shown as sticks. SF3B1, SF3B3, SF3B5, and PHF5A are colored as in Figure 1.

**Figure S2. Structural rearrangements of the SF3B core complex in the presence of pladienolide B (PB). Related to Figure 2.**

(A) Superposition of the SF3B1 and PHF5A SF3B subunits in the presence and absence of the PB ligand. SF3B1 and PHF5A from the PB co-crystal structure are coloured light blue and pink, respectively, while the subunits from the apo SF3B core structure (PDB 5IFE) are coloured dark purple. The individual HEAT repeats of SF3B1 are labelled H1-H20. PB is depicted as sticks and is coloured orange. PHF5A's Zn atoms are indicated as spheres. (B) Superposition of the SF3B3-SF3B5 module of the SF3B core in the presence and absence of PB. SF3B3 and SF3B5 subunits are coloured as in Figure 1, while the SF3B3-SF3B5 module from the apo structure (PDB 5IFE) is in dark purple. The engineered SF3B3 has a shorter insertion loop in the 6th blade of the BPC  $\beta$ -propeller domain as a result of the removal of residues 1068-1085. (C), (D) Comparison of SF3B1 and PHF5A crystal structures at the PB binding site. The SF3B1 HEAT domain and PHF5A from the apo SF3B core structure (PDB 5IFE) are depicted as cartoons and are coloured in dark purple. The PB ligand is represented as orange sticks. SF3B1 and PHF5A subunits from the PB co-crystal structure are coloured light blue and pink, respectively. Key SF3B1 and PHF5A residues lining the PB binding tunnel are shown as sticks. SF3B1-K1071, SF3B1-R1074, and SF3B1-R1075 residues from the SF3B1-PHF5A tunnel are rearranged to accommodate the ligand (arrows), while PHF5A-Y36A and PHF5A-R38 residues adopt similar positions in both crystal structures. (E) Cartoon representation of SF3B1 and PHF5A subunits from the apo SF3B core crystal structure (PDB 5IFE) coloured according to the local B-factors (blue-green-red). Note that HEAT repeat H16 shows higher B factors compared to the neighbouring HEAT repeats of SF3B1. (F) Cartoon representation of SF3B1 and PHF5A subunits from the SF3B-PB co-crystal structure coloured according to their local B-factors (blue-green-red). The PB ligand (orange spheres)

binds SF3B1 in the proximity of the H16 repeat, apparently stabilizing this more dynamic region of SF3B1.

**Figure S3. Chemical structures of SF3B modulators. Related to Figures 3 and 4.**

(A) Representative compounds belonging to the pladienolide (PB), herboxidiene (GEX1A), and spliceostatin (SSA) families of splicing modulators are shown. All compounds share a common diene group (light green) which connects two larger moieties, specific for each family of modulators. Herboxidienes have in common with pladienolides a similar aliphatic arm and with spliceostatins a 6-membered functionalized pyran ring. Chemical groups required for the activity of the compounds are highlighted in purple. (B) Structures of PB derivatives used in this study.

**Figure S4. Structural comparison of the human SF3B-PB co-crystal structure with the yeast SF3B core. Related to Figure 5.**

(A) Three different views of the human SF3B-PB structure superimposed onto the yeast SF3B core in the activated spliceosome. Human SF3B subunits are coloured and displayed as in Figure 1A. The yeast SF3B core (containing the Hsh155p HEAT domain, Rse1p, Rds3p, Ysf3p) is coloured dark purple. PB is depicted as orange spheres. Note that SF3B3, with the exception of its flexible BPB domain, SF3B1 H16-H20, PHF5A, and SF3B5 superimpose onto the yeast proteins without major clashes. The H1-H15 arch of SF3B1 behaves largely as a rigid body with respect to the SF3B1 (H16-H20)-PHF5A-SF3B3 (BPA-BPC)-SF3B5 module and is arranged differently in the two structures. (B) Superposition of PHF5A onto Rds3p as part of the SF3B1 (H16-H20)-PHF5A-SF3B3 (BPA-BPC)-SF3B5 module. Note that PHF5A residues located at the PB binding tunnel (Y36, V37, R38) face the same side, but adopt different conformations in the two structures. (C) Superposition of SF3B5 onto Ysf3p as part of the SF3B1 (H16-H20)-PHF5A-SF3B3 (BPA-BPC)-SF3B5 module. (D) Superposition of SF3B1 (H16-H20), SF3B5, and PHF5A onto the yeast SF3B core (dark purple) as part of the SF3B1 (H16-H20)-PHF5A-SF3B3 (BPA-BPC)-SF3B5 module. Note that the major difference between the two structures results from the different arrangement of the SF3B1 H1-H15 arch with respect to the SF3B1 (H16-H20)-PHF5A-SF3B3 (BPA-BPC)-SF3B5 module. SF3B3 is not shown. (E) Comparison of SF3B1's intramolecular interfaces between consecutive pairs of HEAT repeats in the SF3B-PB and yeast SF3B core structures. The largest difference between the two structures was detected at the H15-H16 interface (r.m.s.d. = 2.06, 66 C $\alpha$ ). Corroborated by the higher B-factor values (Figure S2F), this reveals the location of the hinge region. (F), (G) Structural superpositions of the H15-H17 hinge regions of SF3B1 (blue) and Hsh155p (dark grey), shown in two different orientations (left and right). PB is omitted for clarity sake and the BS-A is shown as sticks (green). PHF5A and the *S. cerevisiae* orthologue are coloured pink and light grey, respectively. SF3B1 residues that belong to the PB-binding site and the equivalent residues from Hsh155p are depicted in blue and dark purple, respectively.

**Figure S5. Addition of PB to purified spliceosomal B complexes has no substantial effect on their ability to catalyse pre-mRNA splicing in the presence of MN-treated extract. Related to Figure 5.**

(A) RNA composition of the affinity-purified B complexes. RNA was analyzed by denaturing PAGE and visualized by staining with silver. B complexes formed on <sup>32</sup>P-labelled MINX-MS2 pre-mRNA were affinity purified as described in the Online Methods. Asterisk, RNA in the loading well of the gel. The presence of the U1, U2, U4, U5, and U6 snRNAs confirms that spliceosomal B complexes were isolated. (B) Purified B complexes were incubated at 30°C for the indicated times (0, 30, 60 min) under splicing conditions in the presence of buffer alone (lanes 1-3) or micrococcal nuclease-treated HeLa nuclear extract (MNNext) (lanes 4-14). PB (1.5 or 6 μM) was added directly to the purified B complexes, followed by a 30 min incubation on ice, prior to performing the chase with MN-treated extract (lanes 6-9) or PB (6 μM) was added to the MN-treated extract (lanes 10-11). As a control for complete MN-digestion, no splicing was observed when <sup>32</sup>P-labelled MINX-MS2 pre-mRNA was incubated with MNNext (lanes 12-14). RNA was analysed by denaturing PAGE and visualized with a Phosphorimager. The positions of the pre-mRNA, splicing intermediates and products are indicated on the right. The % mRNA formed (quantitated with a Phosphorimager) is indicated below selected lanes. Addition of PB had no substantial effect on the ability of B complexes to catalyse splicing after chasing with MNNext. This is consistent with the idea that once SF3B has adopted a closed conformation, as observed in the B complex, PB no longer can bind and inhibit splicing.

**Figure S6. Splicing modulators may act as competitive BS antagonists. Related to Figure 6.**

(A) Summary of the substrates and *in vitro* splicing assays carried out in the presence of PB or PB-OH. The IC<sub>50</sub> values were obtained from non-linear regression curve fitting.

(B) The discriminatory action of splicing modulators towards various 3'SS sequences is a consequence of the competition between substrates and modulators for the “open” conformation of SF3B1 (see also Figure 5E). Potent modulators, such as PB, exhibit high affinity for the “open” conformation of SF3B1, inhibiting the transition to the “closed” conformation even for “strong” substrates. Conversely, modulators that display lower affinities for the “open” state of SF3B1, such as PB-OH, can inhibit efficiently only “weak” substrates. PB is colored in orange, while PB-OH is colored in pink. All the other elements are depicted and labeled as in the Figure 5E.